neurogenetics (2019) 20:129–143
https://doi.org/10.1007/s10048-019-00578-1

ORIGINAL ARTICLE

# A pathogenic CtBP1 missense mutation causes altered cofactor binding and transcriptional activity

David B. Beck[1] · T. Subramanian[2] · S. Vijayalingam[2] · Uthayashankar R. Ezekiel[3] · Sandra Donkervoort[4] · Michele L. Yang[5] · Holly A. Dubbs[6] · Xilma R. Ortiz-Gonzalez[7] · Shenela Lakhani[8] · Devorah Segal[9] · Margaret Au[10] · John M. Graham Jr[10] · Sumit Verma[11] · Darrel Waggoner[12] · Marwan Shinawi[13] · Carsten G. Bönnemann[4] · Wendy K. Chung[14] · G. Chinnadurai[2]

Received: 23 October 2018 / Revised: 18 March 2019 / Accepted: 9 April 2019 / Published online: 30 April 2019


## Abstract

We previously reported a pathogenic de novo p.R342W mutation in the transcriptional corepressor *CTBP1* in four independent patients with neurodevelopmental disabilities [1]. Here, we report the clinical phenotypes of seven additional individuals with the same recurrent de novo *CTBP1* mutation. Within this cohort, we identified consistent CtBP1-related phenotypes of intellectual disability, ataxia, hypotonia, and tooth enamel defects present in most patients. The R342W mutation in CtBP1 is located within a region implicated in a high affinity-binding cleft for CtBP-interacting proteins. Unbiased proteomic analysis demonstrated reduced interaction of several chromatin-modifying factors with the CtBP1 W342 mutant. Genome-wide transcriptome analysis in human glioblastoma cell lines expressing -CtBP1 R342 (wt) or W342 mutation revealed changes in the expression profiles of genes controlling multiple cellular processes. Patient-derived dermal fibroblasts were found to be more sensitive to apoptosis during acute glucose deprivation compared to controls. Glucose deprivation strongly activated the BH3-only pro-apoptotic gene *NOXA*, suggesting a link between enhanced cell death and *NOXA* expression in patient fibroblasts. Our results suggest that context-dependent relief of transcriptional repression of the CtBP1 mutant W342 allele may contribute to deregulation of apoptosis in target tissues of patients leading to neurodevelopmental phenotypes.

**Keywords** C-terminal binding protein · CtBP1 · Chromatin modifying complex · Neurodevelopmental disease · p.R342W mutation

## Introduction

The C-terminal binding protein (CtBP) was originally discovered as a cellular protein that interacts with the C-terminal region of adenovirus E1A protein that antagonizes Ras-induced oncogenesis [2, 3]. Vertebrate genomes code for two different CtBP paralogs that exhibit a high degree of sequence homology [reviewed in ref. [4]]. The major nuclear isoforms of CtBP1 (CtBP1-L, NM_001328.2) and CtBP2 (CtBP2-L, NM_022802.2) function as transcriptional corepressors (reviewed in [5]). CtBPs recruit both DNA-binding repressors and chromatin modifying enzymes through a high-affinity protein-binding interface (PXDLS-binding cleft) (Fig. 1). Besides the PXDLS-binding cleft, a secondary binding interface (RRT-binding groove) is also involved in interacting with certain Zn-finger transcription factors. The enzymatic constituents of the CtBP1 corepressor complex mediate coordinated histone modifications by deacetylation and methylation of histone H3-Lysine 9 and demethylation of histone H3-Lysine 4 [6]. In addition to the transcriptional repression activity, CtBPs have been reported to exert developmental context-dependent transcriptional activation [7–11]. CtBP1 can form homodimers and heterodimers with CtBP2; however, the importance of these interactions has yet to be elucidated. Specifically, many transcriptional activities of

David B. Beck, T. Subramanian, Wendy K. Chung and G. Chinnadurai contributed equally to this work.

**Electronic supplementary material** The online version of this article (https://doi.org/10.1007/s10048-019-00578-1) contains supplementary material, which is available to authorized users.

✉ Wendy K. Chung
wkc15@cumc.columbia.edu

✉ G. Chinnadurai
g.chinnadurai@health.slu.edu

Extended author information available on the last page of the article

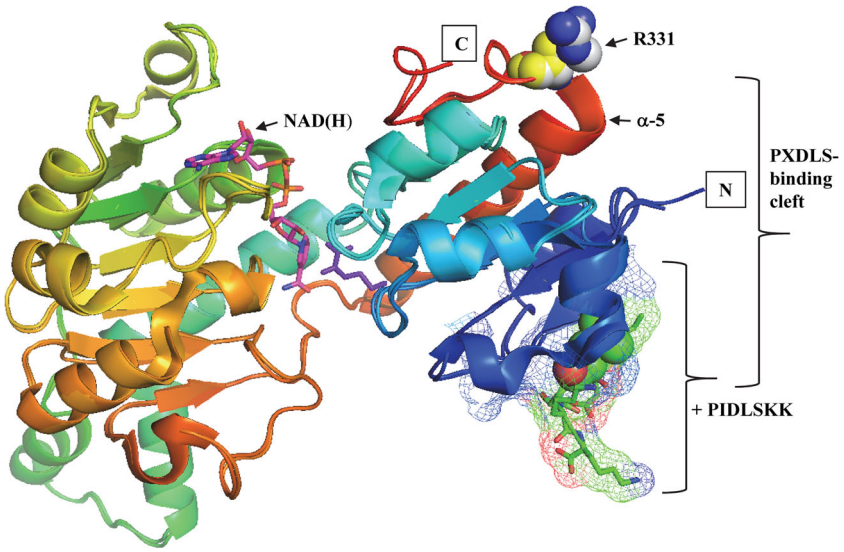


**Fig. 1** The structure of CtBP1(S) bound to a PXDLS containing model peptide. The NAD(H)-binding domain and the PXDLS-binding cleft are indicated. The mutation W342 observed in patients with developmental delays is shown by the arrow (R331 of CtBP1-S, short isoform of CtBP1) that is located within the α-5 region (C-terminal part of the PXDLS-binding cleft). The structure of the PXDLS binding cleft bound to the model peptide PIDLSKK is shown. The Protein Data Bank accession codes are 1hl3 and r1hl3sf [16]

CtBP proteins appear to be associated with CtBP dimers; others have been associated with oligomeric [7, 12–14] and monomeric forms [15]. CtBPs act as metabolic sensors due to their structural similarity to D-isomer-specific 2-hydroxy acid dehydrogenases (D2-HDH), and they employ the dehydrogenase fold for dimerization by complexing with NAD(H) dinucleotides [16, 17]. Since CtBPs bind with NADH more avidly than NAD(+) [18], the nuclear ratio of NAD+/NADH appears to regulate the transcriptional activity of CtBP via conformational changes that influence interactions with cofactors and dimerization/oligomerization status. Thus, CtBPs function as metabolically regulated transcription factors resulting in altered transcriptional profiles with changes in oxidation-reduction activities in the cell.

Studies in mice have indicated that the two *Ctbp* genes play both overlapping and unique transcriptional roles during development [19]. Homozygous deletion of the *Ctbp2* gene is embryonic lethal beyond E10.5 while homozygous deletion of *Ctbp1* results in viable mice with reduced size and lifespan. The developmental and oncogenic activities of CtBPs have been linked to transcriptional regulation of genes that control cell differentiation and apoptosis (reviewed by [4, 20, 21]. A recurrent de novo missense mutation in *CTBP1* (c.991C > T, R331W in NM_001012614.1; R342W c.1024 C > T in NM_001328.2) was recently identified to cause a genetic disorder characterized by developmental delay, intellectual disability, ataxia, hypotonia, and tooth enamel defects in four unrelated patients (MIM: 617915). More recently, Sommerville et al. [22] identified an additional patient with the same mutation and an overlapping phenotype although noted to have progressive neurodegenerative disease with evidence of mitochondrial dysfunction. All reported patients are heterozygous for the p.R342W mutation. Since healthy individuals with heterozygous loss of function alleles have been reported, these mutations likely act through either as a dominant negative or gain of function rather than loss of function mechanism.

The R342W mutation is located in the C-terminal region of CtBP1 that constitutes the substrate-binding cleft, in conjunction with the N-terminal region [16, 17]) (Fig. 1). The substrate-binding cleft is also involved in high-affinity interaction with various CtBP-binding proteins that contain binding motifs related to the prototypical binding motif PXDLS found in the E1A protein [3]. The PXDLS-binding cleft plays an essential role in recruiting various chromatin-modifying components and interacting with different transcriptional regulators [15]. The R342 residue is located in juxtaposition to α-5 sequences that appear to tightly pack against the rest of the substrate-binding domain [16, 17]. The discovery of the recurrent R342W mutation raises the possibility that this residue might be critical in regulating α-5 function, and thereby protein interaction partners. In this manuscript, we report seven additional individuals with the same de novo *CTBP1* p.R342W missense mutation and neurodevelopmental phenotypes to further characterize their clinical condition. We also have determined the effect of the R342W mutation (referred here as W342) on the interaction of various transcriptional regulators and the effect on transcription of select CtBP1-target genes.

## Materials and methods

### DNA extraction and exome sequencing

Genomic DNA was extracted from whole blood. Exome sequencing was performed on exon targets captured using the Agilent SureSelect Human All Exon V4 (50 Mb) kit. After automated filtering of variants with a minor allele frequency (MAF) of > 10%, manual curation was performed to filter less common variants with MAF of 1–10% and variants in genes inherited from unaffected parents, evaluating predicted effects

of rare variants and known function of the genes and associated human conditions, and examining overlapping phenotypes of individuals with de novo variants in the same gene as previously described.

### Cells, plasmids, and antibodies

The glioblastoma cell line (HTB17) was purchased from ATCC and grown in DMEM supplemented with 10% fetal bovine serum. The human dermal fibroblasts from patients [1] and heathy donors were received from Columbia University, Department of Pediatrics and Medicine, and were grown in DMEM supplemented with 10% fetal bovine serum. The cDNA coding for human CtBP1 was cloned into the lentiviral vector, pCDH-CMV-MCS-EF1-Puro (System Biosciences, Mountain View, CA) with 3XFlag tag at the N-terminus and the mutation; W342 was introduced into the lentiviral vector by oligonucleotide-directed mutagenesis. Lentiviruses were prepared using standard protocols and used to infect HTB17 cells. Infected cells were selected for puromycin resistance to establish pooled cell lines. The expression of ectopically expressed CtBP1protein was confirmed by Western blot analysis. The following antibodies were used in this study; Flag antibody agarose and Flag mAb from Sigma, antibodies specific to CoREST1, CtBP1, CtBP2 from BD Biosciences; antibodies to REST, G9a, and ZNF217 from Abcam; antibodies for ZEB1, BIK, and HDAC2 from Santa Cruz Biotechnology; anti-LSD1 from Bethyl Laboratories, anti-BAK and anti-BAX from Upstate Biotechnologies, anti-NOXA from Cell Signaling and rabbit anti-BCL-2 was raised against a synthetic peptide of human BCL-2. Patient-derived fibroblasts were cultured from a 3-mm punch skin biopsy.

### Proteomic analysis and Western blotting

HTB17 glioblastoma cells expressing 3XFlag-CtBP1, mutant W342, or the vector were grown in preparative quantities and collected by centrifugation (5.0 ml pellet volume) and lysed in lysis buffer (20 mM Tris pH 7.9, 0.5 mM EDTA, 10% glycerol, 300 mM KCl. 5 mM MgCl2, 1 mM DTT, 0.1% Tween 20, 0.25 mM PMSF and protease inhibitor cocktail). The lysates were cleared with protein A agarose beads and the proteins were immunoprecipitated with anti-Flag agarose beads. The beads with protein complexes were collected, washed four times with the wash buffer, and subjected to trypsin digestion and LC-MS mass spectrometric analysis (Danforth Plant Research Center, St. Louis). All MS/MS samples were analyzed using Mascot (Matrix Science, London, UK; version 2.5.1). Mascot was set up to search the Uni human database (unknown version, 68,997 entries) assuming the digestion enzyme stricttrypsin. Mascot was searched with a fragment ion mass tolerance of 0.60 Da and a parent ion tolerance of 20 PPM. Oxidation of methionine, acetyl of the n-terminus, and carbamidomethyl of cysteine were specified in Mascot as variable modifications.

Scaffold (version Scaffold 4.8.3, Proteome Software Inc., Portland, OR) was used to validate MS/MS-based peptide and protein identifications. Peptide identifications were accepted if they could be established at greater than 95.0% probability to achieve an FDR less than 1.0% by the Scaffold Local FDR algorithm. Protein identifications were accepted if they could be established at greater than 99.0% probability and contained at least one identified peptide. Protein probabilities were assigned by the Protein Prophet algorithm [23]. Proteins that contained similar peptides and could not be differentiated based on MS/MS analysis alone were grouped to satisfy the principles of parsimony. The mass spectrometry proteomics data have been deposited to the ProteomeXchange Consortium via the PRIDE [1] partner repository with the dataset identifier PXD012702 and https://doi.org/10.6019/PXD012702.

An aliquot of immunoprecipitated samples and lysates were separated by 4–12% gradient gels, transferred to nitrocellulose membrane and incubated at 4 °C overnight with various antibodies. The blots were washed and incubated with the corresponding secondary antibodies conjugated with horseradish peroxidase (Santa Cruz) for 30 min. The blots were then washed and the protein bands were visualized with Western blotting detection system (Roche) according to the manufacturer's specifications. Among the apoptosis-related proteins, NOXA was not detected by Western blotting. Therefore, we immunoprecipitated the cell extracts with NOXA antibody and carried out Western blotting in three independent experiments.

### Glucose deprivation and cell death assay

Normal control dermal fibroblasts and patient fibroblasts were plated in duplicate in 35-mm dishes and incubated at 37 °C for overnight. Next day, cells were washed with phosphate-buffered saline (PBS) and one set of cells were fed with glucose-free DMEM (Invitrogen) supplemented with 10% dialyzed fetal bovine serum (Invitrogen). The other set of cells were fed with normal DMEM supplemented with 10% fetal bovine serum. The cells were incubated at 37 °C for 5–7 days. At the end of experiments, cells were photographed. The second set of cells was stained with DAPI for 10 min, photographed, and quantified. In the third set of experiments, cells were stained with Annexin V and PI using an apoptosis detection kit and analyzed by FACS.

### RNA sequencing and RT-qPCR

HTB17 cells expressing CtBP1 R342 or W342 and the fibroblasts were grown in 150-mm dishes. The cells were washed with PBS and RNA was isolated using TRIzol reagent (Invitrogen). RNA samples were quantitated using Nanodrop and cDNA was synthesized from 2 μg of RNA

using oligo(dT) primer and RT kit (high capacity RNA-to-cDNA kit, Invitrogen) according to the manufacturer's specification. Real-time qPCR was performed with 50 ng of cDNA using TaqMan gene expression master mix, TaqMan primers, and probes (Invitrogen) as mentioned in manufacturer's instruction manual. The following were the specific primer assay ID used for RT-qPCR: ACTIN (Hs99999903_m1), NOXA (Hs00560402_m1), BIK (Hs00609636_m1), BAX (Hs00180269_m1), BAK (Ss03373472_m1), BIM (Hs00708019_s1), MCL1 (Hs01050896_m1), BCL2 (Hs00608023_m1), P21 (Hs01040810_m1), PERP (Hs00751717_s1), CITED1 (Hs00918445_g1), MXD1 (Hs00965581_m1), ENG (Hs00923996_m1), ZNF69 (Hs00737054_m1), and ZNF107 (Hs01598135_mH). All samples were run in triplicate on the Applied Biosystems™ QuantStudio™ 5 Real-Time PCR System and the data analysis done in Thermo Fisher Connect™ (Cloud) https://www.thermofisher.com/us/en/home/digital-science.html

Relative quantification was performed using the RQ App in cloud with Actin as endogenous and reference control is mentioned in the legend. RQ settings–Plot type -RQ Vs Target, Graph Type–Linear, Analysis Type–Singleplex, Confidence Level–95, Benjamini-Hochberg false discovery rate for *P* value–On and Maximum allowed Ct–40.

RNA-seq and analysis was performed in the Saint Louis University Genomics Core. Ribosomal RNA was depleted from total RNA and libraries were constructed using the Eukaryotic RiboMinus and Ion Total RNA-seq v2 kits (Life Technologies, Thermofisher) according to the manufacturer's directions. Sequencing was performed on an Ion Torrent Proton with a mean read length of ~ 100 nucleotides, and reads were aligned to the hg19 human genome sequence using the TMAP aligner map4 algorithm. Soft-clipping at both 5′ and 3′ ends of the reads was permitted during alignment to accommodate spliced reads, with a minimum seed length of 20 nt. The nucleotide coverage for all non-redundant exons was calculated and normalized to total exon coverage using custom scripts in R (R Core Team (2013). R: A language and environment for statistical computing. R Foundation for Statistical Computing, Vienna, Austria. ISBN 3-900051-07-0, URL http://www.R-project.org/). Expression values are total normalized nucleotide exon coverage per gene. Fold changes in gene expression, *p* values, and *q* values were calculated using custom R scripts and Microsoft Excel. Biological process gene ontology analysis was performed using DAVID [24]. RNA-seq data is deposited in the NCBI GEO database.

## Statistical analysis

All analyses were performed in three independent experiments. All data were analyzed using GraphPad Prism 5 software and are presented as the mean ± standard error of the mean. Differences between groups were analyzed via one-way analysis with post hoc contrasts by Student-Newman-Keuls multiple comparison test. $P < 0.05$ was considered to indicate a statistically significant difference.

# Results

## Clinical characterization of patients with the *CTBP1* p.R342W mutation

We present here the clinical profiles of 12 individuals with a heterozygous p.R342W *CTBP1* variant (Table 1) (MIM: 617915). Five cases were previously reported (patients 1–4 and 12 in Table 1) [1, 22], while seven additional cases have not been reported. These cases include four females and eight males and range in age from 4 to 21 years of age. Eleven of twelve individuals exhibit cerebellar atrophy, hypotonia, and global developmental delay with initial recognition of neurodevelopmental disease within the first-year life. The cerebellar disease manifestations include dysarthria, ataxia, gait imbalance, and dysmetria. Nine patients have tooth enamel defects with representative images for patient 8 shown in Fig. 2. Five patients have oculomotor apraxia.

Only one patient had an inherited p.R342W mutation from a clinically unaffected mosaic mother while the mutation in all other patients was de novo. Multiple patients had muscle biopsies with two showing evidence of mitochondrial dysfunction, specifically Complex I deficiency, thought to be secondary to underlying disease. No evidence of myopathy was identified in other patients. Of note, four patients experienced regression of motor milestones and two of these patients also experienced regression in language and cognition. None of the patients had a history of seizures. Together, these additional cases show that *CTBP1*-related disease primarily manifests as cerebellar disease, hypotonia, and enamel defects and highlight the critical role of a single arginine residue in CtBP1 in human development.

## Interaction of CtBP1 corepressor components

In order to understand the mechanisms that contribute to the clinical phenotypes, we first modeled the heterozygous R342W mutation in an established cell culture systeml. We introduced lentiviral constructs that express CtBP1 R342 or mutant W342 in a human glioblastoma cell line, HTB17. Since this mutation is located juxtaposed to α-5 that might regulate cofactor interaction with the PXDLS-binding cleft, we analyzed the interaction of various cofactors with CtBP1 in cells expressing affinity (Flag)-tagged versions of CtBP1 R342 or mutant W342. The protein complexes were immunoprecipitated with the Flag antibody and analyzed by LC/MS analysis (Fig. 3a). The interactions of various proteins were further analyzed by Western blot analysis (Fig. 3b, c, supplemental Fig. 1). These analyses revealed interaction of several previously known components of the CtBP

**Table 1** Clinical profiles of CtBP1 mutated patients

| Patient | Age | Gender (M/F) | Global development delay | Enamel defects | Hypotonia | Neurologic exam | Oculomotor apraxia | MRI | EMG/Muscle Biopsy | EEG | Developmental regression | Other | reference |
|---|---|---|---|---|---|---|---|---|---|---|---|---|---|
| 1 | 10 | M | + | enamel defect | ++ | dysarthria, ataxia, weakness | not reported | mild volume loss of cerebellum, residual white matter changes | evidence of myopathy, fiber splitting, necrosis, no clear evidence of neuropathy | NP | None | Intermittent weakness spells with resolution | [1] |
| 2 | 23 | M | + | soft enamel with discoloration | ++ | ataxia, dysarthria, decreased muscle strength in upper and lower extremities; increased reflexes in LE | + | cerebellar atrophy with progression on MRI | NP | NP | None | Intermittent weakness spells with resolution | [1] |
| 3 | 9 | F | + | wide spaced incisors, brown discoloration of primary incisors | + | ataxia, dysarthria, muscle weakness, exercise intolerance, areflexia, hyperflexibility, tremors | + | superior cerebellar vermis is small, uncertain if this represents volume loss or hypoplasia. Superior vermis is more involved (smaller) than the superior hemispheres. No atrophy of brainstem, including the brachium pontis, or the spinal cord. | NP | normal | None | | [1] |
| 4 | 12 (deceased) | F | + | enamel hypoplasia | + | ataxia | + | MRI normal | | normal | None | | [1] |
| 5 | 20 | M | + | ND | + | ataxia | ND | not received | EMG: Needle exam showed fibrillation activity and a | | None | | |

**Table 1** (continued)

| Patient | Age | Gender (M/F) | Global development delay | Enamel defects | Hypotonia | Neurologic exam | Oculomotor apraxia | MRI | EMG/Muscle Biopsy | EEG | Developmental regression | Other | reference |
|---|---|---|---|---|---|---|---|---|---|---|---|---|---|
| | | | | | | | | | recruitment pattern of motor unit potentials c/w myopathic process. | | | | |
| 6 | 22 | F | + | protuberant malpositio-ned teeth, widely spaced incisors, brown discolor-ation of the roots | + | Limb-girdle and bulbar weakness, significantly decreased muscle bulk and tone throughout, areflexia, bilateral plantar extensor reflexes, bradykinetic movements and speech, wide-based gait requiring support to take steps, moderate contractures of the hips, knees, and elbows, microcephaly | present, horizontal nystag-mus on lateral gaze | progressive, significant cerebellar volume loss over 10 years (10, 22 yoa). Mild enlargement of cerebral sulci, suggesting cerebral volume loss. Myelination age--appropriate. Normal gray white matter differentiation. | EMG: Bilateral ulnar mononeuropat-hies | EEG: mild diffuse back-ground slowing | Slow regression of motor and language function | | [22] |
| 7 | 6 | M | + | dental enamel defect | + | dysarthria, ataxia, muscle weakness | ND | Normal brain MRI at age 3 years | none | normal | None | | |
| 8 | 6 | M | + | enamel dysplasia | + | low tone, absent to areflexia in arms and legs. He was mildly hyperextensi-ble at the | ND | Cerebellar atrophy primarily involving the superior aspect of the cerebellum | EMG is indicative of a diffuse mild to moderate chronic non-irritable myopathy. | NP | None | | |

**Table 1** (continued)

| Patient | Age | Gender (M/F) | Global development delay | Enamel defects | Hypotonia | Neurologic exam | Oculomotor apraxia | MRI | EMG/Muscle Biopsy | EEG | Developmental regression | Other | reference |
|---|---|---|---|---|---|---|---|---|---|---|---|---|---|
| | | | | | | major joints and there was no ankle clonus. Babinski signs were present bilaterally. | | and the vermis was seen on the first study and again on the second study without interval change. | | | | | |
| 9 | 10 | M | + | yes, unspecified, multiple cavities | + (axial) | axial hypotonia, increased tone at ankles, ataxia, wide based gait, difficulty with balance, absent reflexes at knees and ankles, 1+ brachioradial-is weakness in hands and lower extremities | ND | at age 7 yo: mild enlargement of the cisterna magna and hypoplasia of the inferior cerebellar vermis, consistent with a mild Dandy Walker cyst; at age 9 superior cerebellar vermis volume loss | None | normal | Motor, Cognitive | | |
| 10 | 5 | M | + | ND | + | low tone, ataxia, dysarthria | None | Cerebellum was underdevel-oped and has not changed. | None | normal | Motor | | |
| 11 | 11 | M | + | discolored dental enamel, crowded dentition, | + | low tone, ataxia, dysarthria, marked truncal ataxia when standing, finger-to-nose dysmetria bilaterally, rapid alternating movement very slow and dysrhythmic | + | Significant vermian atrophy and to lesser extent bihemispheric cerebellar volume loss with associated volume loss of the superior and inferior cerebellar peduncles as | NP | NP | None | Intermittent weakness spells with resolu-tion | |

**Table 1** (continued)

| Patient | Age | Gender (M/F) | Global development delay | Enamel defects | Hypotonia | Neurologic exam | Oculomotor apraxia | MRI | EMG/Muscle Biopsy | EEG | Developmental regression | Other | reference |
|---|---|---|---|---|---|---|---|---|---|---|---|---|---|
| | | | | | | | | well as the pons | | | | | |
| | | | | | | ataxic, wide-based gait. Required full support to stand and walk. | | | | | | | |
| 12 | 16 | F | + | ND | + | hypotonia, increased tone at elbows, wrists, knees, ankles | ND | mild cerebellar and brainstem atrophy | NP | NP | Motor, language | | [22] |

*ND* not described, *NP* not performed

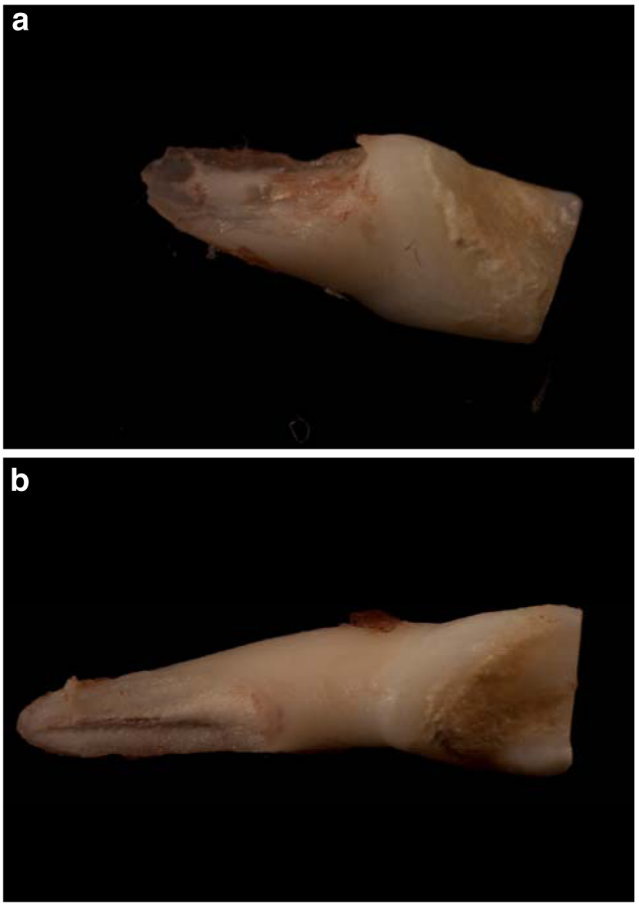


**Fig. 2** Tooth phenotype in a patient. Dental pathology showing root resorption in two different teeth (**a**, **b**) of a patient

corepressor complex. Unbiased proteomic (LC/MS) analysis of the immunoprecipitated samples revealed reduced interaction of various previously validated components of the CtBP1 corepressor complex [6, 15] with CtBP1 W342 compared to CtBP1 R342. These factors included various Zn-finger transcription factors (such as Znf217, ZEB1, ZEB2, and WIZ), histone deacetylases (HDAC1 and 2), histone methyltransferases (G9a and GLA), histone H3-K4 demethylase (LSD-1), and the co-repressor CoREST. Consistent with LC/MS analysis, the Western blot analyses also revealed reduced interaction of various CtBP cofactors with CtBP1 W342. Among the various cofactors, the interaction of HDAC2 with W342 mutant was variable. We note that HDAC2 was shown to exhibit atypical interaction with CtBP2 by interacting with monomeric forms of CtBP2 [25]. These results suggest that the W342 mutation in the α-5 region of the PXDLS-binding cleft may affect the level of cofactor recruitment by CtBP1.

## Effect on genome-wide transcription

In order to examine whether reduced interaction of various CtBP1-associated transcription factors might alter the

**a**

| # | Proteins | Mol. wt in kDa | Peptides | |
|---|---|---|---|---|
| | | | R342 | W342 |
| 1 | CTBP1 | 48 | 176 | 193 |
| 2 | CTBP2 | 49 | 129 | 101 |
| 3 | ZNF-516 | 124 | 54 | 26 |
| 4 | ZNF-217 | 115 | 59 | 13 |
| 5 | ZNF-462 | 285 | 45 | 10 |
| 6 | ZEB-1 | 124 | 23 | 15 |
| 7 | ZEB-2 | 136 | 29 | 14 |
| 8 | LSD-1 | 95 | 55 | 20 |
| 9 | HDAC-1 | 55 | 25 | 18 |
| 10 | HDAC-2 | 55 | 18 | 10 |
| 11 | WIZ | 103 | 39 | 14 |
| 12 | CoREST | 53 | 24 | 11 |
| 13 | EHMT-1 | 141 | 43 | 5 |
| 14 | EHMT-2 | 132 | 35 | 3 |
| 15 | TBB-3 | 50 | 43 | 0 |
| 16 | Q5T0I-1 | 26 | 12 | 0 |
| 17 | H2A2A | 14 | 11 | 7 |

**b**

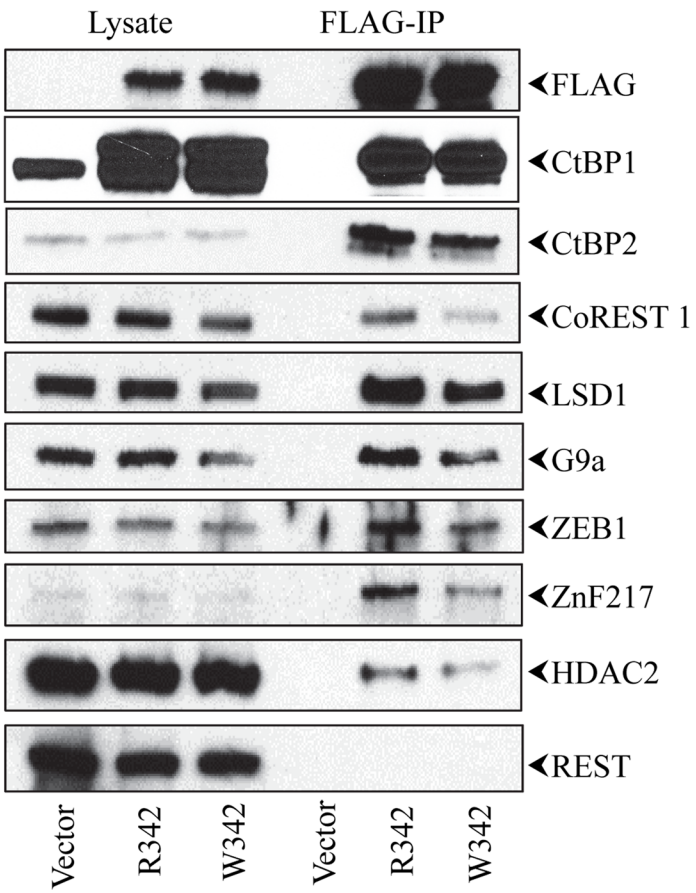


**Fig. 3** Proteomic analyses of CtBP1 and W342 mutant. HTB17 cell lines expressing CtBP1 R342 or mutant W342 with Flag tag or the vector were lysed, pulled with Flag antibody and subjected to LC-MS mass spectrometric analysis. **a** The experiment was repeated twice and the proteomics data are available in ProteomeXchange Consortium via the PRIDE [1] partner repository with the dataset identifier PXD012702 and https://doi.org/10.6019/PXD012702". The results are presented in the supplemental file. From our results, we have selected several known CtBP1 interacting proteins and presented here. The average number of peptides of each protein present in the complexes of CtBP1 R342 and W342 mutant is shown. The names of the proteins with their corresponding molecular weights are given. **b** Western blot analysis of CtBP1 interacting proteins. An aliquot of the immune-affinity purified (IP) samples and lysates were separated by 4–12% gradient gels and analyzed by Western blotting. The experiments were repeated 3 times and the protein levels were determined using Image Studio Litesoftware, LI-COR Biosciences and the relative interactions were calculated (**c**). The relative level of protein interaction to R342 is normalized to 1.0. The *P* values were determined by comparing the interaction of specific protein with R342 to W342: $*P < 0.05$, $**P < 0.01$. Since there was no detectable interaction of CtBP1 with REST, we are unable to quantitate the interaction

transcriptional patterns of CtBP1-target genes, we carried out genome-wide RNA-seq analysis of coding and non-coding RNAs from HTB17 cells that express CtBP1 R342 or W342 mutant. These results revealed similar overall transcriptional profiles between the two cell lines. However, significant ($q < .05$) increases (red) and decreases (blue) in multiple RNA species were detected in W342 cells relative to R342 cells (Fig. 4a). The changes significantly altered multiple biological processes as shown by gene ontology analysis (Fig. 4b, c). Our transcriptome data did not reveal significant differences in the expression of most genes including previously known CtBP-target genes. Since we observed enhanced cell death in patient fibroblasts during glucose deprivation, we examined the expression of known CtBP-target apoptotic genes by qRT-PCR. Quantitative RT-PCR analysis of selected differentially deregulated genes was in general agreement with RNA-seq data (Fig. 4d). However, these data were insufficient to identify specific pathways deregulated in the glioblastoma cell model. Consistent with this, we did not observe differences in the *in vitro* growth characteristics between the two glioblastoma cell models,which were present in patient fibroblast cell lines.

## Deregulation of cell death in patient fibroblasts

We obtained dermal fibroblasts from two patients and two age matched healthy controls (NT011 and LE028) and patients (CSC43 and 44) to analyze cell growth and proliferation. At baseline, the growth and proliferation characteristics of these

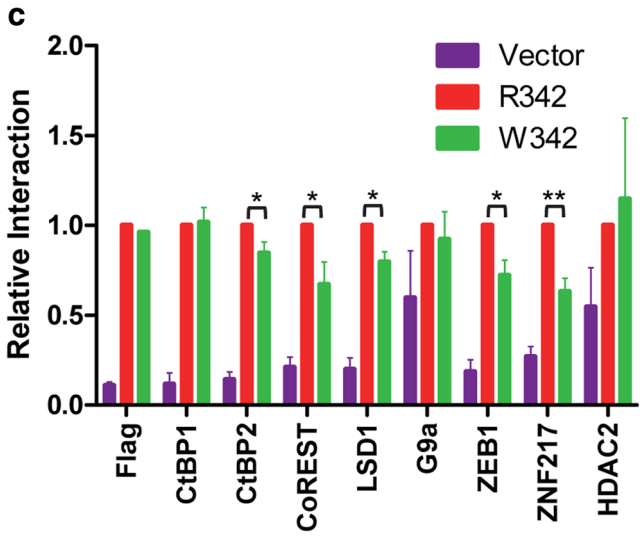


**Fig. 3** continued.

cells did not differ between control and patient fibroblasts (in glucose containing growth media). Since the transcriptional activity of CtBP1 is strongly influenced by the metabolic status of the cells, we rationalized that the mutant allele might exhibit exaggerated differential activity under metabolic stress. We then compared the normal and mutant fibroblasts that were deprived of glucose for 5–7 days. The mutant fibroblasts exhibited strikingly more cell death compared to the normal fibroblasts as revealed by microscopic examination (Fig. 5a), quantification of dead cells stained with DAPI (4′,6-Diamidino-2-phenylindole dihydrochloride) (Fig. 5b), and FACS analysis of cells stained with propidium iodide (PI) and Annexin V (Fig. 5c).

Since several pro-apoptotic genes (such as *Bax*, *Bik*, and *Noxa*) have previously been identified as targets for CtBP1/2 ([26, 27], we carried out q-RT PCR analysis of RNA from control and patient fibroblasts with or without glucose deprivation (Fig. 6a). These results revealed that in control fibroblasts, expression of the transcript for BH3-only pro-apoptotic molecule Noxa was enhanced 8- to 10-fold under glucose starvation compared to cells that were maintained under normal glucose. These results were comparable to a previous report on the effect of glucose starvation on Noxa expression [28]. However, the level of Noxa mRNA expression in glucose-starved patient fibroblasts was more than 30-fold higher compared to patient cells with glucose. To determine the effect of glucose starvation on Noxa protein expression, we carried out immunoprecipitation (IP) and Western blot analysis (Fig. 6b) (endogenous Noxa protein was not detectable in fibroblasts by Western blot analysis of total cell extracts; data not shown). Consistent with the results on the increased levels of Noxa mRNA, higher levels of Noxa protein were detected by immunoprecipitation and Western blot analyses in patient fibroblasts that were exposed to glucose

**Fig. 4** Gene expression profiling of W342 mutant in HTB17 cells by RNA seq analysis. **a** The log2 fold-change in RNA level with the W342 mutant relative to CtBP R342 is plotted against the log2 total expression level in CtBP R342 cells. Expression values are total normalized nucleotide coverage per gene. Red dots indicate genes that are expressed at higher levels in W342 mutant cells than in wt CtBP cells ($q \leq 0.05$) and blue indicates genes that are expressed at lower levels. The RNA seq results were submitted to data bank, and the geo accession number is GSE126253. **b** Biological process ontology analysis of genes expressed at higher levels in W342 cells. **c** Biological process gene ontology analysis of genes expressed at lower levels in W342 cells. **d** Examples of upregulated and down regulated genes. Reference control used in this experiment is HTB17CtBP1 RNA

starvation. In addition to the effect on Noxa, q-RT PCR analysis also revealed varying levels of activation of other pro-apoptotic molecules such as *Bax*, *Bik*, and *Bim*, as well as the anti-apoptotic molecules *Bcl-2*. However, Western blot analysis did not reveal consistent changes in the protein amounts for these genes (Fig. 6b). Thus, our results identify Noxa as a specific target pro-apoptotic target molecule deregulated by the *CTBP1* mutant allele.

## Discussion

As expected from the structure of CtBP1 [16, 17], R342W mutation may affect stable association of various transcriptional regulatory proteins with the PXDLS-binding cleft. Consistent with this interpretation, we have observed reduced levels of interaction of various chromatin-modifying factors such as HDAC1/2, HMTases (G9a and GLA) and H3-K4 demethylase LSD1, the scaffolding protein Co-REST as well as several zinc-finger transcription factors such as ZEB1/2 in unbiased proteomic analysis and by Western blotting (Fig. 3). The expression of the mutant protein in the glioblastoma cell model also resulted in altered expression profiles of genes involved in multiple cellular pathways. Similar to our glioblastoma cell model, we did not detect major differences in the *in vitro* growth phenotypes of patient fibroblasts compared to control fibroblasts. However, when exposed to glucose deprivation, the patient fibroblasts expressed elevated transcript and protein levels of the pro-apoptotic molecule *Noxa* that resulted in increased cell death. Thus, our study has identified *Noxa* as a transcriptional target gene for the CtBP1 mutant allele in human fibroblasts (Fig. 6). Noxa was originally identified as one of the pro-apoptotic CtBP-target genes in mouse fibroblasts derived from *ctbp*1/2 double knockout embryos [29].

*Noxa* expression was increased under glucose deprivation, suggesting that the transcriptional repression activity of CtBP1 might be relieved in cells that express the mutant allele under bioenergetic changes resulting from glycolysis inhibition. As cellular NADH levels affect the association of CtBP

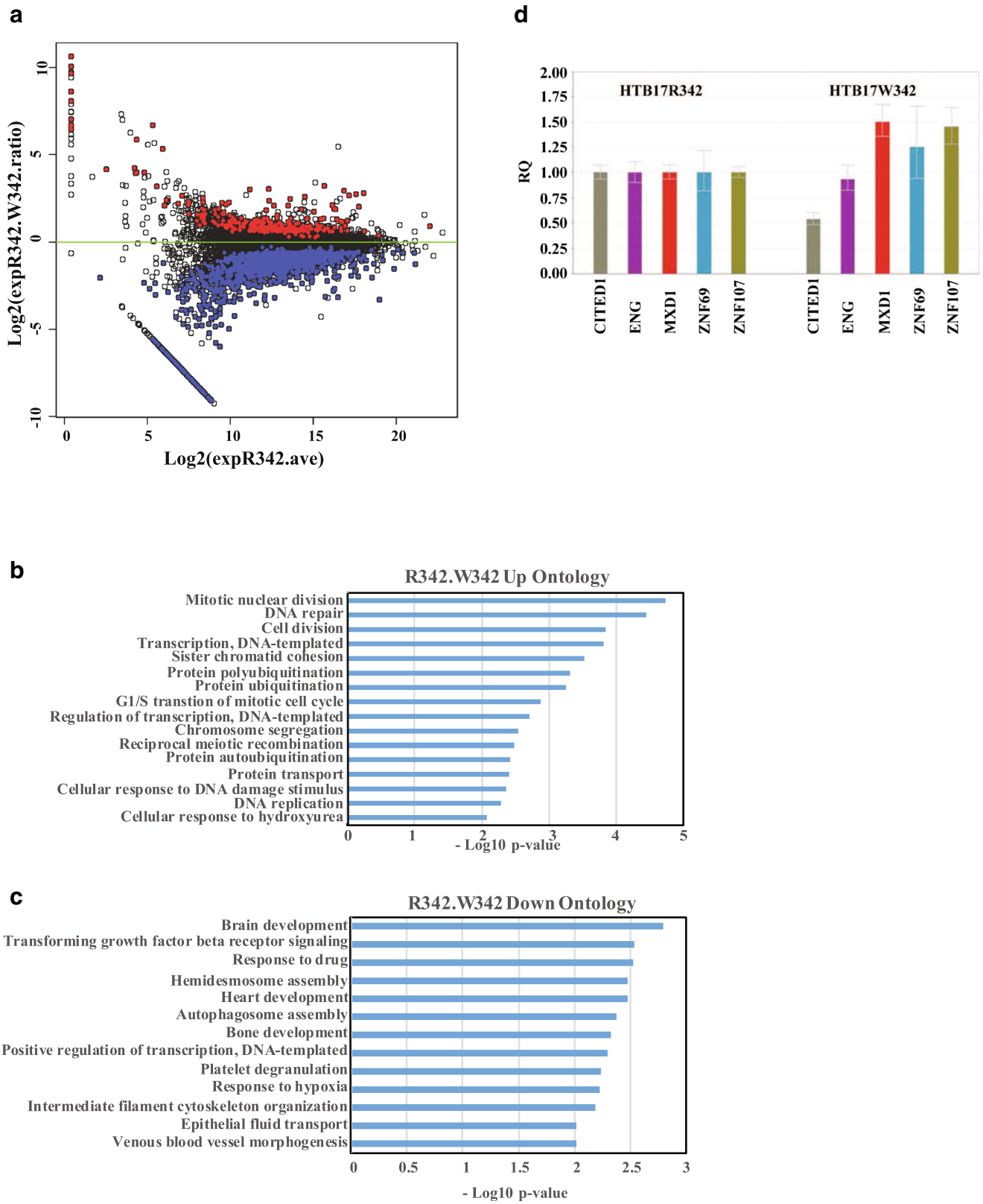


with cofactors via dimerization and oligomerization [18], reductions in NADH caused by glucose deprivation may contribute to the relief of transcriptional repression by the mutant allele. We also noted the CtBP1 mutant W342

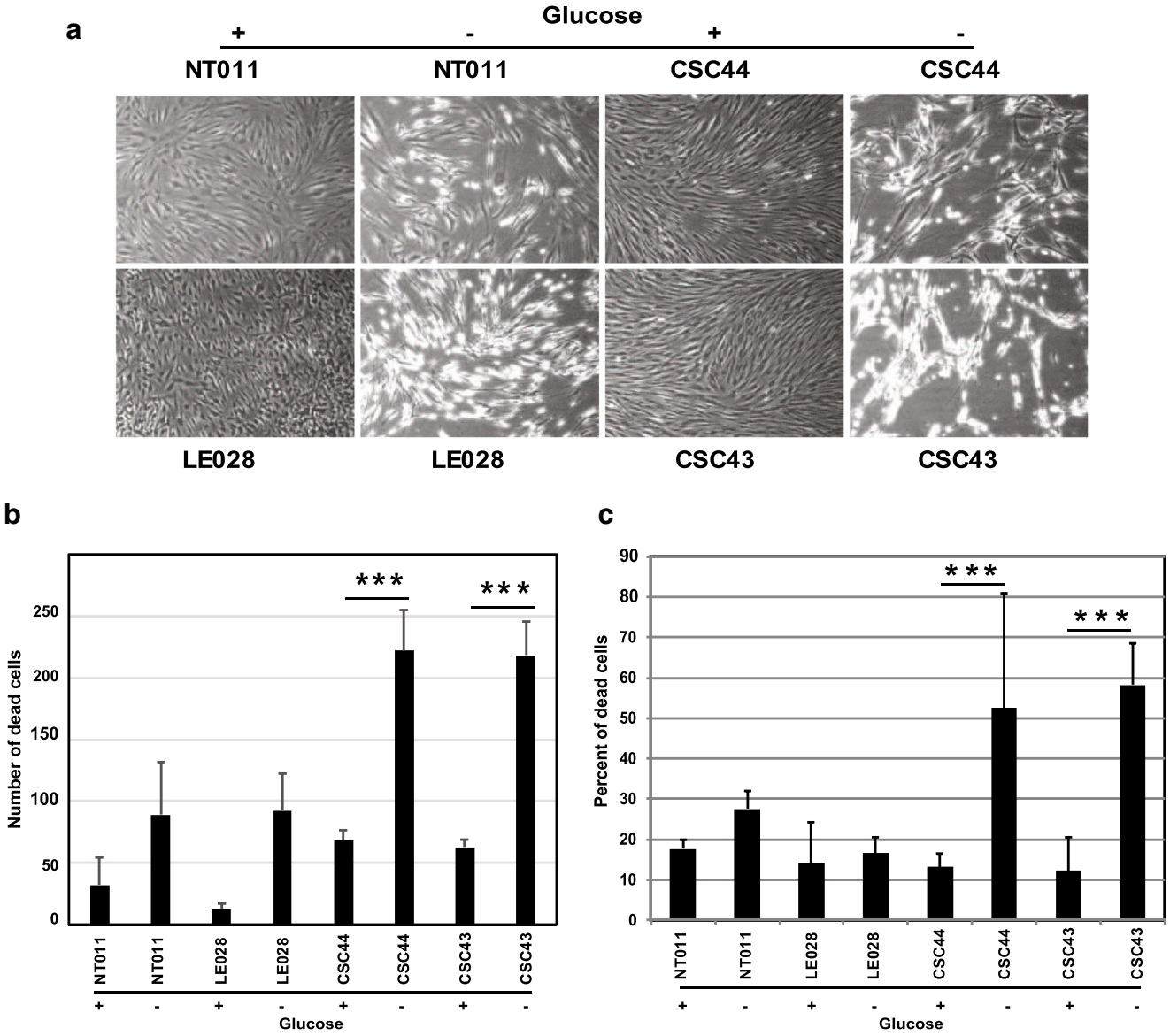


**Fig. 5** Effect of glucose deprivation on cell death. Dermal fibroblasts from normal donors (NT011 and LE028) and patients (CSC43 and 44) were grown in media containing normal media (indicated by +) or media lacking glucose (indicated by −) for 6 days. The cells were photographed under phase contrast (**a**) or quantitated under fluorescence microscope after staining with DAPI (**b**). Cells were also stained with Annexin V and PI using an apoptosis detection reagents and analyzed by FACS (**c**). The experiments were repeated 3 times and the average number and percentage of cell death with standard deviation was plotted. The *P* values were determined by comparing the cell death in the presence and absence of glucose in growth medium:***$P < 0.001$

interacted with various binding partners at reduced levels even under normal glucose conditions (Fig. 3). Thus, W342 mutation may affect the association of CtBP-binding proteins even in the presence of glucose. However, reduction in the levels of NADH with glucose deprivation may exaggerate the defect. In addition, glucose deprivation in patient cells with primary or secondary mitochondrial dysfunction may also lead to increased cell death which may, in part, explain the phenotype. associated with CTBP1 mutations. These results raise the possibility that the *de novo CTBP1* mutation p.R342W may contribute to developmental phenotypes as a result of deregulated apoptosis in affected regions of the brain such as the cerebellum where CtBP1 is highly expressed (www.proteinatlas.org/ENSG00000159692-CTBP1/tissue).

There are multiple reports of heterozygous frameshift mutations in unaffected individuals [30], suggesting that one wild-type allele of *CtBP1* is sufficient for normal neurodevelopment and that haploinsufficiency is not the disease mechanism present in these cases. The number of independent recurrent *de novo* mutations of the same missense mutation with overlapping phenotypes suggest significant specificity of the effect of this alteration. Our results combined

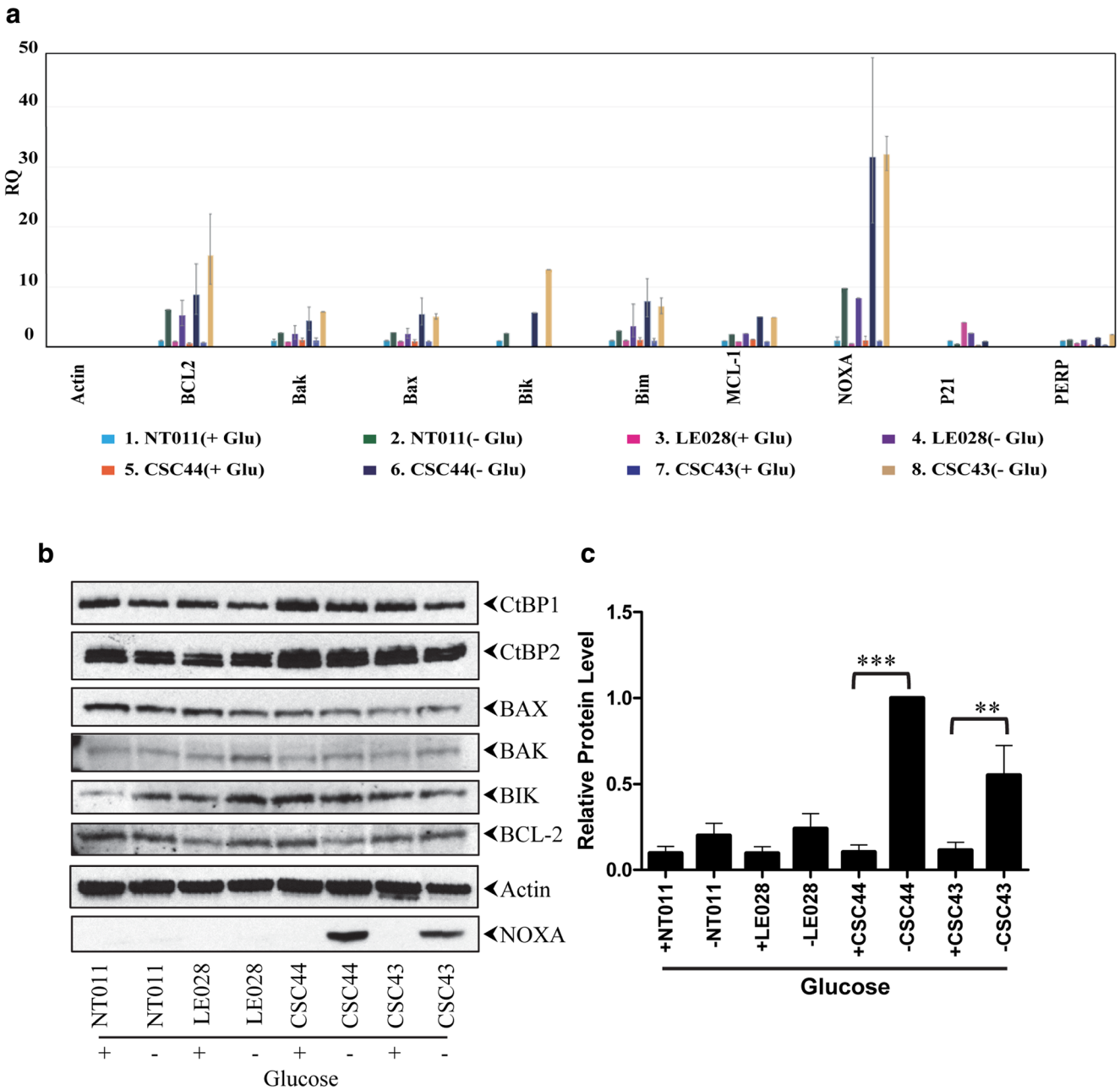


**Fig. 6** Effect of glucose deprivation on the expression of apoptotic and anti-apoptotic genes. **a** RNA analysis by RT-qPCR. The experiment was carried out in triplicate and the relative quantification (RQ) values are plotted. Reference control used in this experiment is NT011(+ Glu)RNA. **b** Western blot analysis of apoptosis-related proteins. To detect NOXA, cell extracts were immunoprecipitated and analyzed by Western blotting. + indicates cells in glucose media. – indicates cells in media lacking glucose. The experiment was repeated 3 times and quantitated the relative protein level using Image Studio Lite software, LI-COR Biosciences (**c**). The relative level of expression of NOXA in CSC44 cells in medium lacking glucose is normalized to 1.0. The *P* values were determined by comparing the expression of NOXA in the presence and absence of glucose in growth medium: $^{**}P < 0.01$, $^{***}P < 0.001$

with the known autosomal dominant mode of inheritance of the *CtBP1* p.R342W mutation suggest different binding of the W342 allele [1]. Interestingly, *CtBP2* has a highly conserved PXDLS motif and with a neighboring arginine which is not mutated in the healthy population. It is possible that similar mode of disease will be shown for this paralog and that *CTBP1* and *CTBP2* may function together in disease. In spite of the predictions, it remains to be determined whether the mutant allele indeed functions in a dominant negative fashion in patient cells to activate *Noxa*. Future, studies with patient-derived lineage specific cell models may illuminate the detailed mechanistic basis leading to manifestation of different phenotypes.

**Acknowledgments** We thank the families for their generous contributions. We thank CureCMD and Anne Rutkowski with their help in patient recruitment.

**Funding** This work was supported by an ICTS pilot grant from Washington University in St. Louis and Presidential Research support from Saint Louis University. This work was supported in part by grants from the JPB Foundation and the Simons Foundation. Work in C.G. Bönnemann's laboratory is supported by intramural funds from the NIH National Institute of Neurological Disorders and Stroke. M.Y. is supported by the following industry sponsored research: Reveragen, Italfarmaco.

## Compliance with ethical standards

**Conflict of interest** The authors declare that they have no conflict of interest.

**Ethical approval** All procedures performed in studies involving human participants were in accordance with the ethical standards of the institutional research committee and with the 1964 Helsinki Declaration and its later amendments or comparable ethical standards.

**Informed consent** Informed consent was obtained from all individual participants included in the study.

## References

1. Beck DB, Cho MT, Millan F, Yates C, Hannibal M, O'Connor B, Shinawi M, Connolly AM, Waggoner D, Halbach S, Angle B, Sanders V, Shen Y, Retterer K, Begtrup A, Bai R, Chung WK (2016) A recurrent de novo CTBP1 mutation is associated with developmental delay, hypotonia, ataxia, and tooth enamel defects. Neurogenetics 17:173–178
2. Boyd JM, Subramanian T, Schaeper U, la Regina M, Bayley S, Chinnadurai G (1993) A region in the C-terminus of adenovirus 2/5 E1a protein is required for association with a cellular phosphoprotein and important for the negative modulation of T24-ras mediated transformation, tumorigenesis and metastasis. EMBO J 12: 469–478
3. Schaeper U, Boyd JM, Verma S, Uhlmann E, Subramanian T, Chinnadurai G (1995) Molecular cloning and characterization of a cellular phosphoprotein that interacts with a conserved C-terminal domain of adenovirus E1A involved in negative modulation of oncogenic transformation. Proc Natl Acad Sci U S A 92:10467–10471
4. Chinnadurai G (2002) CtBP, an unconventional transcriptional corepressor in development and oncogenesis. Mol Cell 9:213–224
5. Chinnadurai G (2007) Transcriptional regulation by C-terminal binding proteins. Int J Biochem Cell Biol 39:1593–1607
6. Shi Y, Sawada JI, Sui G, Affar EB, Whetstine JR, Lan F, Ogawa H, Po-Shan Luke M, Nakatani Y, Shi Y (2003) Coordinated histone modifications mediated by a CtBP co-repressor complex. Nature 422:735–738
7. Fang M, Li J, Blauwkamp T, Bhambhani C, Campbell N, Cadigan KM (2006) C-terminal-binding protein directly activates and represses Wnt transcriptional targets in drosophila. EMBO J 25: 2735–2745
8. Itoh TQ, Matsumoto A, Tanimura T (2013) C-terminal binding protein (CtBP) activates the expression of E-box clock genes with CLOCK/CYCLE in drosophila. PLoS One 8:e63113
9. Paliwal S, Ho N, Parker D, Grossman SR (2012) CtBP2 promotes human Cancer cell migration by transcriptional activation of Tiam1. Genes Cancer 3:481–490
10. Ray SK, Li HJ, Metzger E, Schule R, Leiter AB (2014) CtBP and associated LSD1 are required for transcriptional activation by NeuroD1 in gastrointestinal endocrine cells. Mol Cell Biol 34: 2308–2317
11. Bajpe PK et al (2013) The corepressor CTBP2 is a coactivator of RAR/RXR in retinoic acid signaling. Mol Cell Biol 33(16):3343–3353
12. Bhambhani C, Chang JL, Akey DL, Cadigan KM (2011) The oligomeric state of CtBP determines its role as a transcriptional coactivator and co-repressor of wingless targets. EMBO J 30:2031–2043
13. Madison DL, Wirz JA, Siess D, Lundblad JR (2013) Nicotinamide adenine dinucleotide-induced multimerization of the co-repressor CtBP1 relies on a switching tryptophan. J Biol Chem 288:27836–27848
14. Bellesis AG, Jecrois AM, Hayes JA, Schiffer CA, Royer WE Jr (2018) Assembly of human C-terminal binding protein (CtBP) into tetramers. In: J biol Chem, vol 293, pp 9101–9112
15. Kuppuswamy M, Vijayalingam S, Zhao LJ, Zhou Y, Subramanian T, Ryerse J, Chinnadurai G (2008) Role of the PLDLS-binding cleft region of CtBP1 in recruitment of core and auxiliary components of the corepressor complex. Mol Cell Biol 28:269–281
16. Nardini M, Spanò S, Cericola C, Pesce A, Massaro A, Millo E, Luini A, Corda D, Bolognesi M (2003) CtBP/BARS: a dual-function protein involved in transcription co-repression and Golgi membrane fission. EMBO J 22:3122–3130
17. Kumar V, Carlson JE, Ohgi KA, Edwards TA, Rose DW, Escalante CR, Rosenfeld MG, Aggarwal AK (2002) Transcription corepressor CtBP is an NAD(+)-regulated dehydrogenase. Mol Cell 10: 857–869
18. Zhang Q, Piston DW, Goodman RH (2002) Regulation of corepressor function by nuclear NADH. Science 295:1895–1897
19. Hildebrand JD, Soriano P (2002) Overlapping and unique roles for C-terminal binding protein 1 (CtBP1) and CtBP2 during mouse development. Mol Cell Biol 22:5296–5307
20. Byun JS, Gardner K (2013) C-terminal binding protein: a molecular link between metabolic imbalance and epigenetic regulation in breast Cancer. Int J Cell Biol 2013:647975
21. Dcona MM, Morris BL, Ellis KC, Grossman SR (2017) CtBP- an emerging oncogene and novel small molecule drug target: advances in the understanding of its oncogenic action and identification of therapeutic inhibitors. Cancer Biol Ther 18:379–391
22. Sommerville EW, Alston CL, Pyle A, He L, Falkous G, Naismith K, Chinnery PF, McFarland R, Taylor RW (2017) De novo CTBP1 variant is associated with decreased mitochondrial respiratory chain activities. Neurol Gen 3:e187
23. Nesvizhskii AI, Keller A, Kolker E, Aebersold R (2003) A statistical model for identifying proteins by tandem mass spectrometry. Anal Chem 75:4646–4658
24. da Huang W, Sherman BT, Lempicki RA (2009) Systematic and integrative analysis of large gene lists using DAVID bioinformatics resources. Nat Protoc 4:44–57
25. Zhao LJ, Kuppuswamy M, Vijayalingam S, Chinnadurai G (2009) Interaction of ZEB and histone deacetylase with the PLDLS-binding cleft region of monomeric C-terminal binding protein 2. BMC Mol Biol 10:89
26. Grooteclaes ML, Frisch SM (2000) Evidence for a function of CtBP in epithelial gene regulation and anoikis. Oncogene 19:3823–3828
27. Kovi RC, Paliwal S, Pande S, Grossman SR (2010) An ARF/CtBP2 complex regulates BH3-only gene expression and p53-independent apoptosis. Cell Death Differ 17:513–521
28. Lowman XH, McDonnell MA, Kosloske A, Odumade OA, Jenness C, Karim CB, Jemmerson R, Kelekar A (2010) The proapoptotic

function of Noxa in human leukemia cells is regulated by the kinase Cdk5 and by glucose. Mol Cell 40:823–833

29. Grooteclaes M, Deveraux Q, Hildebrand J, Zhang Q, Goodman RH, Frisch SM (2003) C-terminal-binding protein corepresses epithelial and proapoptotic gene expression programs. Proc Natl Acad Sci U S A 100:4568–4573
30. Lek M et al (2016) Analysis of protein-coding genetic variation in 60,706 humans. Nature 536:285–291



## Affiliations

**David B. Beck[1] · T. Subramanian[2] · S. Vijayalingam[2] · Uthayashankar R. Ezekiel[3] · Sandra Donkervoort[4] · Michele L. Yang[5] · Holly A. Dubbs[6] · Xilma R. Ortiz-Gonzalez[7] · Shenela Lakhani[8] · Devorah Segal[9] · Margaret Au[10] · John M. Graham Jr[10] · Sumit Verma[11] · Darrel Waggoner[12] · Marwan Shinawi[13] · Carsten G. Bönnemann[4] · Wendy K. Chung[14] · G. Chinnadurai[2]**

1 National Human Genome Research Institute, National Institutes of Health, 10 Center Drive, Room B3-4129, Bethesda, MD 20892, USA

2 Institute for Molecular Virology, Department of Molecular Microbiology and Immunology, Saint Louis University School of Medicine, E. A. Doisy Research Center, 6th Floor, St. Louis, MO 63104, USA

3 Clinical Health Sciences, Saint Louis University, 3437 Caroline Street, Allied Health Building, Suite 3025, Saint Louis, MO 63104, USA

4 National Institute of Neurological Disorders and Stroke Neurogenetics Branch, National Institutes of Health, 10 Center Drive Room 2B39, MSC 1477, Bethesda, MD 20892, USA

5 University of Colorado Denver, 13123 E. 16th Ave; Box B155, Aurora, CO 80238, USA

6 Division of Neurology, The Children's Hospital of Philadelphia, Philadelphia, PA 19104, USA

7 Department of Neurology, Pereleman School of Medicine, University of Pennsylvania; Division of Neurology, The Children's Hospital of Philadelphia, Philadelphia, PA 19104, USA

8 Center for Neurogenetics, Brain and Mind Research Institute, Weill Cornell Medicine, 413 E 69th Street, New York, NY 10021, USA

9 Department of Pediatrics, Division of Child Neurology, Weill Cornell Medicine, 525 E. 68th St, Box 91, New York, NY 10065, USA

10 Medical Genetics, Department of Pediatrics, Cedars-Sinai Medical Center, 8700 Beverly Blvd, Los Angeles, CA 90068, USA

11 Division of Pediatric Neurology, Department of Pediatrics, Emory University School of Medicine, Atlanta, GA 30322, USA

12 Department of Human Genetics, University of Chicago, Chicago, IL 60637, USA

13 Department of Pediatrics, Division of Genetics and Genomic Medicine,, Washington University School of Medicine, St. Louis, MO 63110, USA

14 Departments of Pediatrics and Medicine, Columbia University Medical Center, New York, NY, USA>